

# Assessment of Passive Islanding Detection Methods for DC Microgrids

*Ahmad Makkieh*<sup>†</sup>, *Anthony Florida-James*<sup>†</sup>, *Dimitrios Tzelepis*<sup>†</sup>, *Abdullah Emhemed*<sup>†</sup>, *Graeme Burt*<sup>†</sup>  
*Scott Strachan*<sup>†</sup>, *Adria Junyent-Ferre*<sup>\*</sup>

<sup>†</sup>*Department of Electronic & Electrical Engineering, University of Strathclyde, Glasgow, UK, ahmad.makkieh@strath.ac.uk*

<sup>\*</sup>*Department of Electrical Engineering, Imperial College London, London, UK, adria.junyent-ferre@imperial.ac.uk*

**Keywords:** DC microgrid networks, distributed energy resources, distributed control, islanding detection methods.

## Abstract

This paper provides an assessment of passive islanding detection methods in DC microgrids. In order to analyse the response of a DC microgrid to an islanding event, DC voltage and current signatures are captured locally at the terminals of Distributed Energy Resources (DERs). Further analysis on DC voltage and current measurements is carried out to derive the Rate of Change of Voltage (ROCOV) and the Rate of Change of Current (ROCO), to distinguish between genuine islanding events and other disturbances. A detailed DC microgrid has been developed in MATLAB/Simulink to analyse the response of the DERs within a DC microgrid during intentional or unintentional islanding events. The results show that these approaches cannot be used to classify and characterise between islanding and non-islanding events caused by high resistive faults for DC microgrids, as the response of the DERs are dependent on the technology and associated control systems, which influences post event analysis in distinguishing between events.

## 1 Introduction

Recently, DC Microgrids (MGs) have received increased attention in power network research, particularly for small scale commercial and residential applications [1]. DC MGs can offer greater controllability when compared to AC MGs and conventional distribution networks. Further benefits include improved energy efficiency, enhanced power quality, and increased reliability for local consumers [2]. Recent technical research on DC microgrids has focused on fault-related challenges such as DC fault detection, isolation strategies, and reconfiguration the DC network after clearing faults [3–5]. However, there is limited work that has considered islanding detection techniques in DC microgrids. The importance of detecting islanding events in DC MGs, is related to operation, protection and security. When operation in islanding mode is prohibited, as per the grid codes, an islanding event should be detected in order to disconnect the local DER/DG. This is important to ensure that the risk of damaging equipment and human life is diminished. In the case that continuous operation in islanding mode is permitted, an islanding event should also be detected in order to change the DC microgrid protection and

control strategies but also to physically adjust the system (e.g. trigger earthing switches). It should be noted that the detection of islanding events usually refers to the unintentional islanding as, in the case of intentional islanding, the system is obviously already aware of the lack of the AC grid. The performance of any islanding detection scheme is assessed whilst the DC microgrid is within a Non-Detection Zone (NDZ). The NDZ is used as an index, and is defined as the operational power region in which an islanding detection method fails to detect the islanding event [6]. As such the smaller the NDZ index, the greater the capability of the detection scheme. Therefore, the detection scheme must be reliable, robust, and capable of accommodating the transition to intentional or unintentional islanding to ensure reliable and safe operation of the DC microgrid.

This paper assesses the passive islanding detection techniques within a DC microgrid by measuring the DC voltage and current locally at the DERs. The paper is organised as follows: Section 2 provides a review of the different islanding detection methods for DC MGs. The detailed DC microgrid model and the simulation analysis are presented in Section 3. Finally, the conclusions of the presented work are drawn in Section 4.

## 2 Islanding detection methods

To date, research has proposed both passive, active and remote islanding detection methods for AC systems [7]. Unlike AC MG systems, DC MGs have limited islanding detection methods. From a power system point of view, the only measurable parameter that could be naturally disturbed during islanding is the DC voltage. Consequently, most islanding detection methods for AC microgrids (e.g. Rate of Change of Frequency (ROCOF) and different phase-shift based schemes) cannot be applied to DC MGs [8]. Therefore, islanding detection for DC MGs should be based on other parameters, such as DC voltage measurements and subsequent analysis of DC voltage.

### 2.1 Passive detection methods

These methods mainly rely on continuously monitoring the measured system parameters, such as voltage and current. When islanding occurs, if these parameters satisfy an islanding detection criterion (e.g. over/under voltage), the protection devices will detect islanding and initiate a control command

(e.g. disconnect or change to islanding mode). Passive techniques are quite simple and can be very effective when there is a significant power mismatch between generation and demand, prior to islanding [6]. However, the performance of these methods deteriorate if such mismatches are zero or nearly zero, as a large NDZ is inherited [9, 10]. Other passive methods for DC MGs include under/over voltage [11, 12] and autocorrelation function of model current envelope [6].

## 2.2 Active detection methods

Active methods can be only applied to DGs which are interfaced with power electronic converters. Such methods are based on the injection of deliberate disturbances into the DG circuit (i.e., through the converter control scheme). This is based on the fact that when a MG is grid-connected, any injected disturbance will be absorbed by the system and it will not impose any instability. However, after the disturbance, if the system becomes unstable then an islanding event can be detected. Active methods can potentially provide a cheaper approach compared to the passive methods for islanding detection and can significantly reduce the NDZ, due to feedback control techniques that detect changes in the parameters such as the voltage or current at the DG [13, 14]. However, the continuous perturbations in the system can potentially lead to degradation of power quality. Also, in some cases, the detection time can be slower when compared to passive methods [15]. This arises from the control which takes time to analyse the system response during the perturbation process. The most commonly used methods for DC MGs are positive feedback [16], harmonic injection, and insertion of a controllable load methods [17, 18].

## 2.3 Remote detection methods

Remote methods rely on the information exchange between various system components by use of communication links. The information could be the status of circuit breaker (e.g. direct inter-tripping schemes) or any other system variable (e.g. current and voltage). Remote schemes are characterised by high performance when compared to passive and active methods. This is because the NDZ can be effectively zero and at the same time they maintain full immunity to external system disturbances. However, there are high equipment and communication technology costs. Additional challenges include communication failures and cyber security issues [13].

## 3 Simulation-based analysis

This section includes comparative analysis of the MG network transients during genuine islanding events and other disturbances not related to islanding (e.g. load step changes and Fault). A detailed model was built within MATLAB/Simulink to generate the simulation results for the various case studies.

### 3.1 Modelling

The system under study is a typical DC microgrid network as depicted in Figure 1. The DC network comprises of a 0.5 MW PV array, a 1.5 MW battery storage system, and a DC load.

The entire DC network operates at 750 V and is connected to an AC grid supply point through a two-level Voltage Source Converter (VSC) and an 11/0.4 kV transformer.

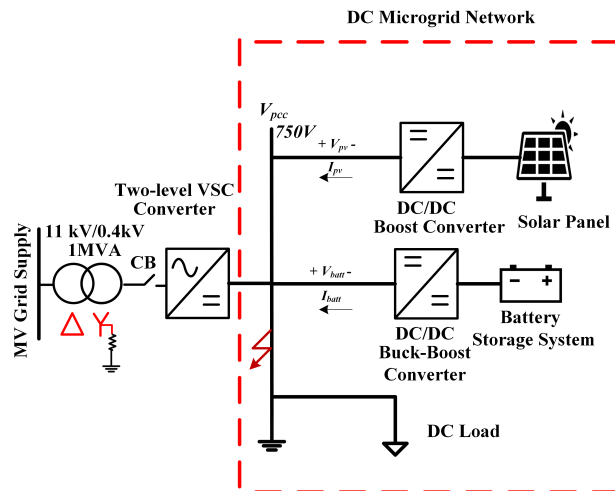


Figure 1: DC microgrid test network.

During steady state grid-connected conditions, the main AC-DC converter operates in DC voltage control mode to maintain the DC voltage at 750V DC. The PV system is interfaced via a DC-DC boost converter and operates using the Maximum Power Point Tracking (MPPT) algorithm (i.e. constant power mode). A buck-boost DC-DC half bridge converter interfaces the 600 Vdc battery storage to the 750 Vdc MG network. Boost mode is activated when the battery operates in the discharge mode, while buck mode is activated when the battery operates in the charge mode. The battery model used in this simulation is the generic Lithium-Ion Battery model found within Simulink library with a nominal voltage of 600 Vdc, and an initial State Of Charge (SOC) of 80%. The simulation time step used in the study was  $5\mu\text{s}$  and the sampling frequency for the signal acquisition was 200 kHz. The DC microgrid test system parameters are illustrated in Table 1.

Table 1: AC and DC network parameters.

Parameter	Value
AC grid Voltage [kV]	11
Transformer voltage ratio [kV]	11/0.4
Transformer rating [MVA]	5
AC frequency [Hz]	50
AC-DC converter rating [MW]	1
DC voltage [V]	750
Battery rating [MW]	1.5
PV rating [MW]	0.5
DC load [MW]	0.371

### 3.2 DC grid control strategies

In order for the battery DC-DC converter to achieve a seamless switch between charging and discharging mode, its operation is driven via a V-I droop control [19], as shown in Figure 2.

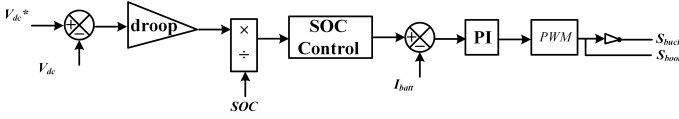


Figure 2: Diagram of the DC current control loop of the battery.

During normal operation, the main VSC converter maintains a constant DC voltage by controlling the power exchange with the AC grid. When the energy capacity is insufficient, the battery can contribute to DC voltage regulation by sharing the power deficit. However, during abnormal conditions, (e.g. losing the AC grid), the power exchange with the AC grid will drop to zero and consequently the VSC control of the DC voltage will be lost. In this case, the battery becomes the only DG in the microgrid to regulate the DC voltage by adjusting the buck-boost switching and injecting or absorbing current. The control strategy adopted for the studies presented in this paper, follows the charge/discharge characteristic depicted in Figure 3.

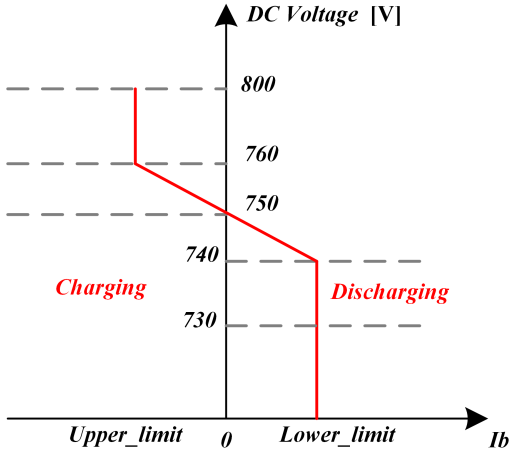


Figure 3: Droop control curve for battery.

Such a control strategy assures that the battery is being charged whenever the DC load demand is less than the total generation capacity (and hence there is an over-voltage). On the contrary, if the DC voltage drops below 750 V (i.e. the demand is higher than the generation) the converter provides voltage droop regulation of the DC bus in the range of 740-750 V. The vertical edges of this curve are the absolute current rating of the battery converter which define as Upper/Lower current limits accordingly.

### 3.3 Scenarios

In order to test the response of the DC MG associated with passive islanding detection methods, various disturbances have been used for analysis. These include a genuine islanding event, a DC-side fault and load step changes (refer to Table 2 for detailed descriptions).

#### 3.3.1 DC-side fault

The pole-to-pole fault scenario is applied at the DC link with high resistive fault, while the DC MG is kept connected to the AC grid.

#### 3.3.2 Loss of main (LOM)

The loss of main scenario (islanding) is taking place at the point of interaction between the AC grid and VSC converter by opening the circuit breaker (CB). In this case, when a network outage occurs, there will be measurable change in voltage at the PCC due to load-generation mismatch.

#### 3.3.3 Load step changes

In case of DC load step changes, the DC load is decreased/increased to 20% of the normal condition, while the DC MG is kept connected to the AC grid.

Table 2: Description of scenarios.

Scenario	Description
LOM	Loss Of Main (DC microgrid in islanding mode)
Fault	Highly, resistive pole-to-pole fault ( $R_f = 3 \Omega$ )
High Load	Load step change of +20 %
Low Load	Load step change of -20 %

Based on these scenarios, DC voltage and current measurements have been captured at each of the DG separately (i.e. PV and battery storage). These measurements were used to calculate ROCOV and ROCOC using equations (1) and (2) respectively.

$$ROCOV = \frac{v(t_k) - v(t_k - \Delta t)}{\Delta t} \quad (1)$$

$$ROCOV = \frac{i(t_k) - i(t_k - \Delta t)}{\Delta t} \quad (2)$$

where,  $v(t_k)$  and  $i(t_k)$  is the measured value of voltage and current at the time of  $k^{th}$  sample and  $\Delta t$  is the simulation time step.

The ROCOV and ROCOC detection methods are based on the real power mismatch between the local load and generation. This mismatch results in deviations or transient in the DC MG current and voltage during islanding mode. The measurements captured during such mismatches can be utilised to characterise and detect islanding behaviour, as load-generation mismatch will occur during this grid connected-islanded transition. Consequently, measuring the ROCOV and ROCOC can be used to distinguish whether the DC MGs are operating within the host grid or in islanded mode. The dynamic change in the voltage and the current is directly proportional to power mismatch at the point of common coupling (PCC) following islanding and can be approximated as in (3) and (4) respectively [20].

$$ROCOV = \frac{V}{2P_L} * \frac{\Delta P}{\Delta t} \quad (3)$$

$$ROCOV = \frac{I}{2P_L} * \frac{\Delta P}{\Delta t} \quad (4)$$

where  $\Delta P$  is the active power imbalance,  $V$  and  $I$  is the terminal voltage and current respectively and  $P_L$  is the active power of the DC load.

As shown in (3) and (4), any power mismatch  $\Delta P$  will cause transients during islanded operation, and consequently the terminal voltage and the current will deviate from their nominal values. However these methods are limited. If the power mismatch  $\Delta P$  during islanded operation is small or nearly zero, then the terminal voltage and the current will change gradually, and is therefore a challenge to distinguish between islanding and non-islanding events.

### 3.4 Simulation results

The simulation results for battery and PV measurements can be seen in Figures 4 and 5 respectively. The different scenarios are triggered at  $t = 0.05\text{ s}$  and the measurements have been averaged using a time window of  $t_w = 40\text{ ms}$ . The passive detection methods have been carried out per occurrence of the scenarios. Figure 4(a) shows the DC voltage at the battery buck-boost converter for the four different scenarios. It can be observed from the results that the DC voltage is maintained at 750V during normal operation. However, the DC voltage is hardly affected during occurrence of the DC-side fault scenario. The changes in DC voltage can be pronounced when ROCOV is derived (shown in Figure 4(b)). It can be observed that the active power mismatch in LOM scenario is small, and result in a small change in the ROCOV over time. It is also important to note that the LOM and the high resistive fault scenarios are almost have same ROCOV at the beginning of each scenario, which mean it is hard to set one threshold to differentiate between these two scenarios. The similarities of DC voltage and ROCOV to these scenarios indicate that plain DC voltage and ROCOV methods might not be suitable to discriminate between LOM scenario and other disturbances and can be so small and potentially undetectable.

In Figure 4(c) the DC current of the battery response is presented for the various scenarios. The response demonstrates the nature of the transient current resulting from the DC-DC converter capacitor discharging during the pole-to-pole fault. During a LOM scenario the battery DC-DC converter control discharges current to maintain the voltage of the DC link. After 50ms the ROCOC is calculated by measuring the currents during the different scenarios. The ROCOC is expected to be high during the LOM scenario. In addition, the LOM and fault scenarios have similar ROCOC behaviour at the beginning of the scenario occurring. This may result in the detection scheme failing to detect LOM from other disturbances in the case of small power mismatch as shown in Figure 4(d). It is important to note that there is a significant difference in the ROCOC for the two different load steps, due to the different direction of current flow. The ROCOC stays around  $\pm 3\text{ kA/s}$ , which slightly reduces over time.

Subsequently, the same four scenarios were used to investigate the effect of the passive detection methods using measurements at the PV DC bus. The voltage and current measurements have been captured at the local DC bus of the PV. The results il-

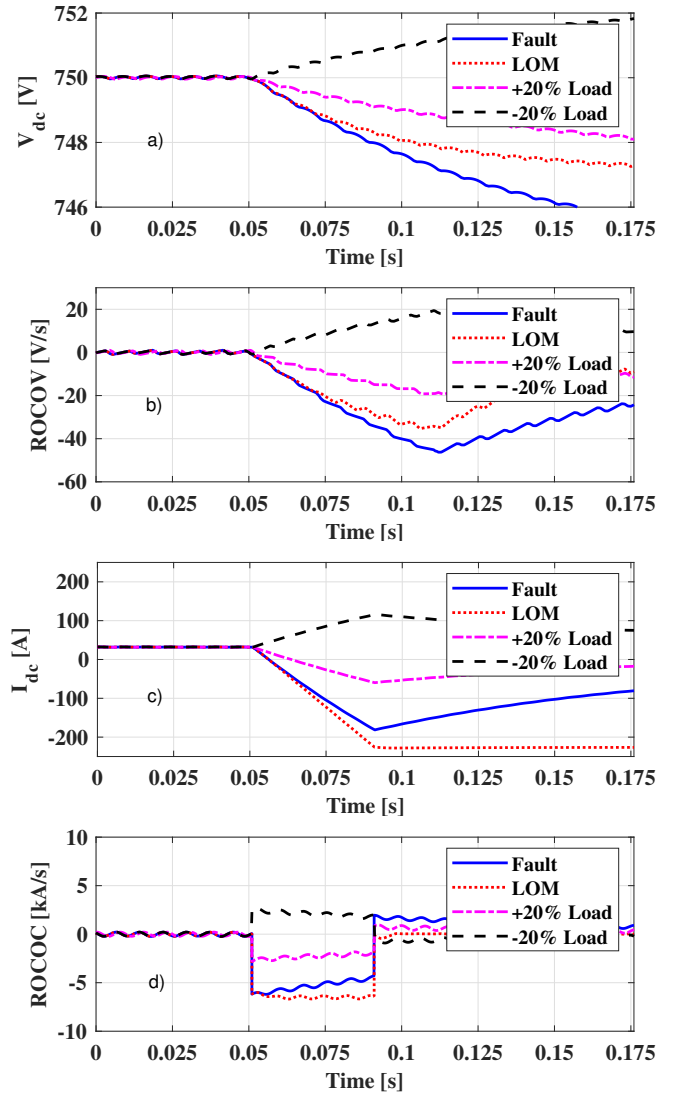


Figure 4: Response of battery system to four scenarios: a)  $V_{dc}$ , b) ROCOV, c)  $I_{dc}$ , d) ROCOC.

lustrated in Figure 5 which are the DC voltage, DC current of the PV array, ROCOV, and ROCOC detection methods. These results clearly demonstrate that DC voltage at the local bus of the PV and the ROCOV method have a similar response to the battery as described previously. However, the DC current and ROCOC method have different response from the battery. During the pole-to-pole fault the DC current of the PV has been increased. This is due to the DC-DC boost converter of the PV not having the capability to limit the fault current. Consequently, the highest ROCOC value is obtained from the high resistive fault scenario, which reaches value close to  $+15\text{ A/s}$  as shown in Figure 5(d). A challenge for those four scenarios would be the discrimination between LOM and fault scenarios as they have similar values for both ROCOV and ROCOC detection methods. The ROCOV and the ROCOC values for both events reach close to  $-20\text{ v/s}$  and  $+10\text{ A/s}$  respectively.

### 3.5 Discussion

Using passive ROCOV and ROCOC methods to discriminate between various scenarios will have different response on the

behaviour of the battery. This is due to power mismatch between the load and the generation. It is clearly noticeable from the results that both passive ROCOV and ROCOC methods are not enough to discriminate between the LOM and fault scenarios. Thus, it is difficult to provide an absolute threshold for detecting islanding detection using ROCOV and ROCOC methods. In addition, the simulation results show that it is difficult to detect LOM scenario by simply observing the ROCOV and ROCOC for the PV. Therefore, there is a significant challenge related LOM detection by using the ROCOV and ROCOC for PV when the load and the generation of islanded distribution network closely match. Additionally, the highest ROCOV and ROCOC values are obtained from high resistive fault scenario compared to other scenarios.

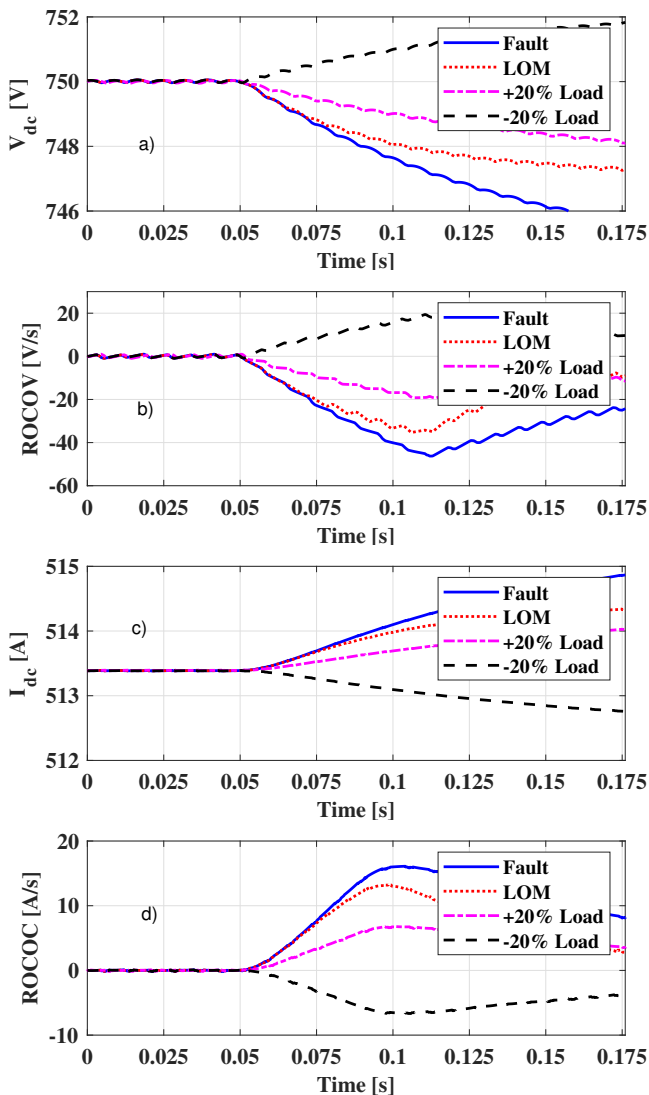


Figure 5: Response of PV system to four scenarios: a)  $V_{dc}$ , b) ROCOV, c)  $I_{dc}$ , d) ROCOC.

## 4 Conclusions

This paper assessed passive detection methods for islanding events, which were utilised locally at the distributed energy resources in the DC microgrid network. A detailed DC MG

model was developed, which used the rate of change of voltage and the rate of change of current based islanding detection methods. The performance of these detection schemes were assessed for different scenarios. The indices of the rate of change of voltage and the rate of change of current were calculated at the local DC terminal of the battery and PV. Based on the voltage, current, ROCOV, and ROCOC waveforms analysis, the following observation can be made:

- In DC microgrids, passive islanding detection methods have limitations, like non-detection zone, as well as hard to discriminate between LOM and high resistive fault.
- Using the rate of change of voltage and the rate of change of current based islanding detection methods for battery and PV can not solely provide a discrimination requirement between islanding and other non-islanding events. This is because the power mismatch between generation and local load is small or nearly zero, while also the power electronic converter based distributed energy sources have different control schemes, which impact on measurements of islanding detection methods.

There is a need for developing an islanding detection method in future DC microgrid since it will be challenging to provide every DERs with remote detection based methods if the number of distributed generation sources connected to DC microgrid will be high. The work presented in this paper demonstrated that passive methods are not suitable for distinguishing between islanding and non-islanding events. Future recommended work includes development of a new passive detection methods, such as travelling wave based islanding detection schemes. These are not computationally demanding and fits well into existing DC-DC converter schemes, such as the one outlined in this paper. Such schemes are also fast in terms of identifying islanding detection with power mismatch for various events.

## References

- [1] H. Kakigano, Y. Miura, and T. Ise, "Low-voltage bipolar-type dc microgrid for super high quality distribution," *IEEE Transactions on Power Electronics*, vol. 25, no. 12, pp. 3066–3075, Dec 2010.
- [2] H. Kakigano, M. Nomura, and T. Ise, "Loss evaluation of DC distribution for residential houses compared with AC system," in *International Power Electronics Conference - ECCE ASIA*, June 2010, pp. 480–486.
- [3] A. A. S. Emhemed, K. Fong, S. Fletcher, and G. M. Burt, "Validation of fast and selective protection scheme for an LVDC distribution network," *IEEE Transactions on Power Delivery*, vol. 32, no. 3, pp. 1432–1440, June 2017.
- [4] S. Mirsaedi, X. Dong, S. Shi, and D. Tzelepis, "Challenges, advances and future directions in protection of hybrid ac/dc microgrids," *IET Renewable Power Generation*, vol. 11, no. 12, pp. 1495–1502, 2017.

- [5] A. Emhemed and G. Burt, "The effectiveness of using IEC-61660 for characterising short-circuit currents of future low voltage DC distribution networks," in *22nd International Conference and Exhibition on Electricity Distribution (CIRED)*, June 2013, pp. 1–4.
- [6] R. Haider, C. H. Kim, T. Ghanbari, S. B. A. Bukhari, M. S. uz Zaman, S. Baloch, and Y. S. Oh, "Passive islanding detection scheme based on autocorrelation function of modal current envelope for photovoltaic units," *IET Generation, Transmission Distribution*, vol. 12, no. 3, pp. 726–736, 2018.
- [7] D. Tzelepis, A. Dyško, and C. Booth, "Performance of loss-of-mains detection in multi-generator power islands," in *13th International Conference on Development in Power System Protection 2016 (DPSP)*, March 2016, pp. 1–6.
- [8] Y. A. R. I. Mohamed, "Analysis and stabilization of active DC distribution systems with positive feedback islanding detection schemes," *IEEE Transactions on Power Electronics*, pp. 1–1, 2018.
- [9] H. Vahedi, R. Noroozian, A. Jalilvand, and G. B. Gharehpetian, "A new method for islanding detection of inverter-based distributed generation using DC-link voltage control," *IEEE Transactions on Power Delivery*, vol. 26, no. 2, pp. 1176–1186, April 2011.
- [10] H. T. Do, X. Zhang, N. V. Nguyen, S. S. Li, and T. T. Chu, "Passive-islanding detection method using the wavelet packet transform in grid-connected photovoltaic systems," *IEEE Transactions on Power Electronics*, vol. 31, no. 10, pp. 6955–6967, Oct 2016.
- [11] C. N. Papadimitriou, V. A. Kleftakis, and N. D. Hatziaargyriou, "A novel method for islanding detection in dc networks," *IEEE Transactions on Sustainable Energy*, vol. 8, no. 1, pp. 441–448, Jan 2017.
- [12] H. H. Zeineldin and J. J. L. Kirtley, "Performance of the ov/ufp and ofp/ufp method with voltage and frequency dependent loads," *IEEE Transactions on Power Delivery*, vol. 24, no. 2, pp. 772–778, April 2009.
- [13] A. M. I. Mohamad and Y. A. R. I. Mohamed, "Assessment and performance comparison of positive feedback islanding detection methods in DC distribution systems," *IEEE Transactions on Power Electronics*, vol. 32, no. 8, pp. 6577–6594, Aug 2017.
- [14] T. Zheng, H. Yang, R. Zhao, Y. C. Kang, and V. Terzija, "Design, evaluation and implementation of an islanding detection method for a micro-grid," Jan 2018.
- [15] K. Ahmad, J. Selvaraj, and N. Rahim, "A review of the islanding detection methods in grid-connected pv inverters," pp. 756 – 766, Jan 2013.
- [16] A. M. I. Mohamad and Y. A. R. I. Mohamed, "Analysis and mitigation of interaction dynamics in active DC distribution systems with positive feedback islanding detection schemes," *IEEE Transactions on Power Electronics*, vol. 33, no. 3, pp. 2751–2773, March 2018.
- [17] V. A. Kleftakis, D. T. Lagos, C. N. Papadimitriou, and N. D. Hatziaargyriou, "Seamless transition between interconnected and islanded operation of DC microgrids," *IEEE Transactions on Smart Grid*, pp. 1–1, 2017.
- [18] D. Voglitsis, N. Papanikolaou, and A. C. Kyritsis, "Incorporation of harmonic injection in an interleaved flyback inverter for the implementation of an active anti-islanding technique," *IEEE Transactions on Power Electronics*, vol. 32, no. 11, pp. 8526–8543, Nov 2017.
- [19] A. Florida-James, S. Yana, A. Emhemed, and G. Burt, "Investigation of a decentralised control strategy for grid frequency support from dc microgrids," in *The 7th International Conference on Renewable Power Generation (RPG2018)*, 2018, pp. 1–6.
- [20] W. Chang, "An islanding detection method for grid-connected inverter of distributed renewable generation system," in *Asia-Pacific Power and Energy Engineering Conference*, March 2011, pp. 1–4.